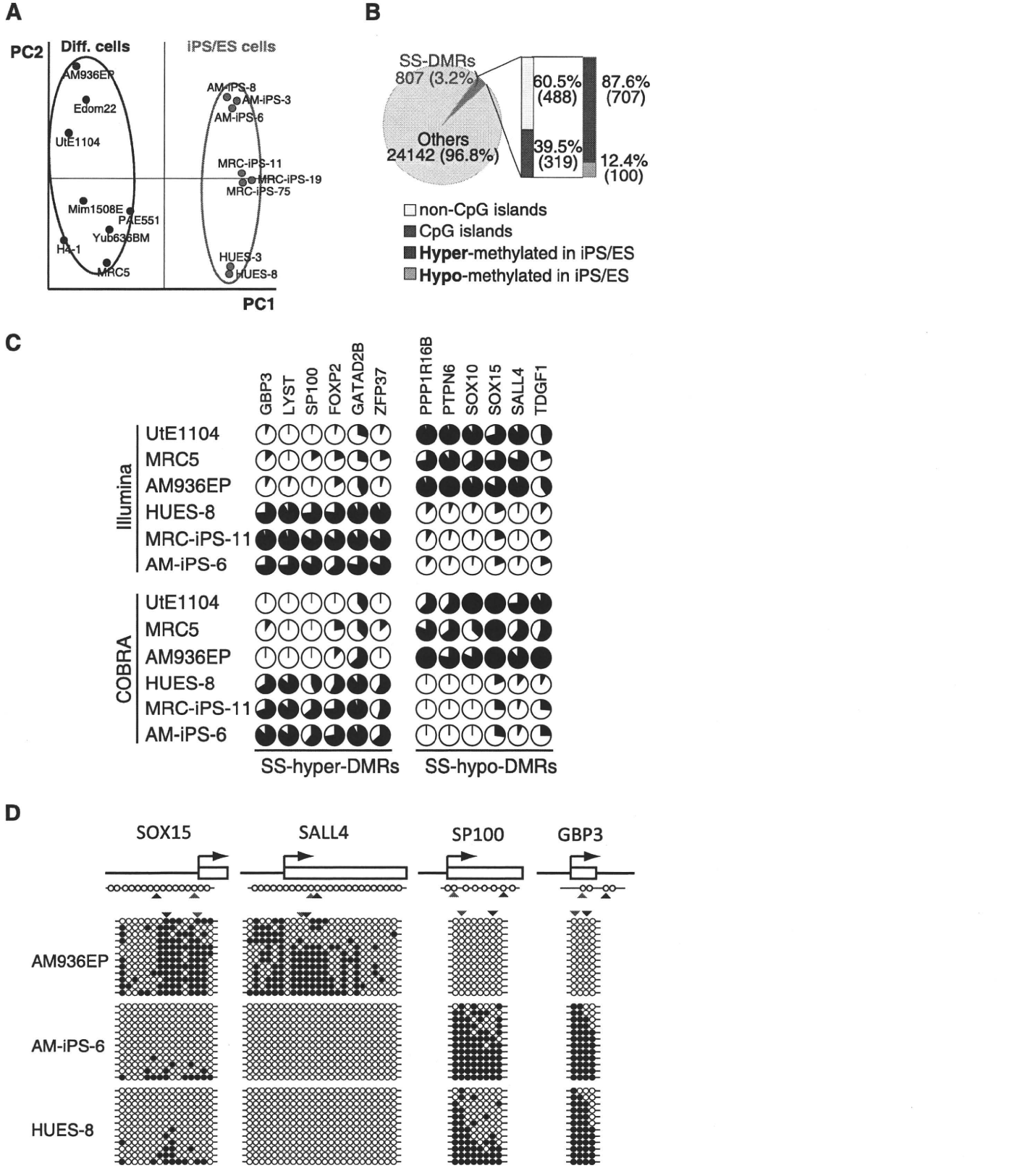

Figure 2. Pluripotent stem cells are significantly more hyper-methylated than differentiated cells. (**A**) Principal component analysis (PCA) for DNA methylation states of 24,949 CpG sites with 16 human cell lines. The PC1 axis clearly distinguish iPS/ES cell group from differentiated cells, while human iPS cells are very close to human ES cells. (**B**) Stem cell-specific differently methylated regions (SS-DMRs) were defined by PC1. In the pluripotent stem cells, 60.5% of the SS-DMRs are located outside of CpG islands and 87.6% of the SS-DMRs are hyper-methylated. (**C**) DNA methylation levels at promoter regions in 12 representative genes determined by Illumina Infinium HumanMethylation27 assay and Bio-COBRA.

Details of these genes are described in Table S6B. The promoter regions of these genes were defined as the SS-DMRs. The relative amount of methylated DNA ratio is indicated as the black area in the pie chart. The same methylation patterns in 12 regions were detected both by Infinium assay and COBRA. (**D**) Bisulfite sequencing analysis of the same regions that were analyzed by Infinium assay and COBRA assay in *SOX15, SALL4, SP100* and *GBP3*. (Top) Schematic diagram of the genes. Arrows, open boxes and open circles represent transcription start site, first exon and position of CpG sites, respectively. (Bottom) Open and closed circles indicate unmethylated and methylated states, respectively. Red and blue arrowheads represent the position of CpG sites in Infinium assay and COBRA, respectively.
doi:10.1371/journal.pone.0013017.g002

aberrant DMSs, 155 sites overlapped between MRC- and AM-iPS cells (Fig. 1F and data set S1, S2, S3). Overlapping aberrant DMSs are located at promoters in genes such as gene for FZD10, MMP9 and three zinc finger proteins (ZNF551, ZNF513 and ZNF540). These genes are hyper-methylated in iPS cells than parental cells and ES cells. Approximately 80% of aberrant DMSs are hyper-methylated, compared with parent cells and ES cells.

Defining stem cell specific differentially methylated regions (SS-DMRs). Principal component analysis (PCA) shows high similarity among human iPS and ES cells and clearly separates the iPS/ES cells from the differentiated cells, which is supported by hierarchical clustering analysis (Fig. 1B and Fig. 2A). Based on principal component 1 (PC1), 807 (3.2%) out of 24,949 sites were deduced to change their methylation state along with "stemness" (Fig. 2B). We designated a region represented by such CpG sites as "stem cell specific differentially methylated regions" (SS-DMRs). Of the 807 SS-DMRs, 39.5% (319 sites) are localized on CpG islands, whereas 60.5% (488 sites) are not (Fig. 2B), although 72.5% CpG sites on the bead-chips occur on CpG islands. Thus, promoter regions on non-CpG islands were more affected during reprogramming towards pluripotent stem cells. 707 sites (87.6%) of the SS-DMRs were significantly increased in the methylation levels in iPS/ES cells, compared with those in the differentiated cells, and we designated these sites as "stem cell specific hyper-differentially methylated regions (SS-hyper-DMRs) " (Fig. 2B and data set S4). In contrast, 100 sites (12.4%) were decreased and designated as "stem cell specific hypo-differentially methylated regions (SS-hypo-DMRs) " (Fig. 2B and data set S5). We also confirmed the methylation state in the promoter regions for some of the detected genes by another means, i.e. quantitative combined bisulfite restriction analysis (COBRA) [15] (Fig. 2C). In addition, results of bisulfite sequencing of the region surrounding the SS-DMRs corresponded to results of Infinium assay and COBRA (Fig. 2D).

Gene ontology analysis with the SS-DMRs. We searched gene ontology databases for details of the SS-DMRs. Interestingly, SS-hypo-DMRs are abundant in genes related to nucleic acid binding and transcription factors, which may function in iPS cells. On the other hands, SS-hyper-DMRs are abundant in genes related to differentiation (Table 2). We also subjected the SS-DMRs to KEGG (Kyoto Encyclopedia of Genes and Genomes) pathway. Cytokine receptor interaction cascade, MAPK signaling, and Neuroactive ligand-receptor interaction are all major keywords for SS-hyper-DMRs (Table S2).

Expression of genes with SS-DMRs in human iPS/ES cells. To address whether changes in DNA methylation state are associated with expression levels, we surveyed genes showing more than 5-fold change of expression in human iPS/ES cells, compared with those in differentiated cells, using the GEO database [16,17]. Twenty-three genes represented by SS-hypo-DMRs were found in "genes significantly expressed in iPS/ES cells" (Table 3 and Table S3A). Representative genes, including *SOX15*, *SALL4*, *TDGF1*, *PPP1R16B* and *SOX10*, are expressed with hypo-methylation states in iPS/ES cells (Fig. 3A). On the other hand, forty-three genes represented by SS-hyper-DMRs were found in "genes significantly suppressed in iPS/ES cells" (Table S3B and S4). Representative genes, *SP100* and *GBP3*, are suppressed by hyper-methylation in iPS/ES cells (Fig. 3A). Among DNA methyltransferases, *DNMT3B* was reported to be highly expressed in human ES cells [18]. *DNMT3A*, *DNMT3B* and *DNMT3L* were indeed expressed in iPS/ES cells (Fig. 3A). The *DNMT3A* promoter in iPS/ES cells became demethylated, while *DNMT3B* and *DNMT3L* promoters remained low methylated during reprogramming (Fig. 3A and Table S5A), leading us to analyze chromatin in iPS/ES cells in addition to DNA methylation.

Histone H3K4 and H3K27 modification of genes with the SS-DMRs. Histone modification is another important mechanism in epigenetics. Methylation of lysine 4 (K4) and 27 (K27) on histone H3 is associated with active and silent gene expression, respectively [19], while bivalent trimethylation (me3) of H3K4 and K27 represses their gene expression in ES cells [20,21]. Based on the database of the UCSC Genome Bioinformatics, the promoter of *DNMT3B* in human ES cells is highly modified by 3K4me3, compared with that in human lung fibroblasts (Table S5B). No differences in histone modification of H3K4me3 or H3K27me3 between ES and lung fibroblasts at promoter of *DNMT3L* were detected (Table S5B). We also compared DNA methylation of the SS-DMRs with reported data for whole-genome mapping of H3K4me3 and H3K27me3 in the promoter regions of human ES cells [22]. In SS-hyper-DMRs, 68.8% do not have trimethylation of H3K4 and K27 (Fig. 3B). On the other hand, 42.3%, 1.3%, and 30.8% of SS-hypo-DMRs are marked with H3K4me3, H3K27me3, and bivalent H3K4me3 and K27me3, respectively (Fig. 3B). Thirteen out of the 23 genes in

Table 2. A list of top 7 categories of GO Term in "SS-DMRs".

Molecular Function		
PantherID: GO Term	**Count. Genes**	**%**
SS-hypo-DMRs		
MF00042:Nucleic acid binding	30	41.10%
MF00036:Transcription factor	15	20.55%
MF00099:Small GTPase	11	15.07%
MF00137:Glycosyltransferase	8	10.96%
MF00082:Transporter	6	8.22%
MF00154:Metalloprotease	6	8.22%
MF00098:Large G-protein	6	8.22%
SS-hyper-DMRs		
MF00213:Non-receptor serine/threonine protein kinase	124	20.98%
MF00262:Non-motor actin binding protein	119	20.14%
MF00001:Receptor	80	13.54%
MF00131:Transferase	76	12.86%
MF00099:Small GTPase	66	11.17%
MF00242:RNA helicase	57	9.64%
MF00261:Actin binding cytoskeletal protein	53	8.97%

doi:10.1371/journal.pone.0013017.t002

Table 3. A list of 23 genes with SS-hypo-DMRs exhibiting 'high' expression in human iPS/ES cells.

TargetID	Gene name	Fold change of expression	DNA methylation level in iPS/ES cells	DNA methylation level in Diff. cells
cg07337598	*ANXA9, annexin A9*	5.53	0.294±0.023	0.712±0.014
cg24183173	*BCOR, BCL-6 interacting corepressor*	5.06	0.014±0.005	0.784±0.051
cg21207436	*C14orf115, hypothetical protein LOC55237*	63.49	0.052±0.005	0.442±0.036
cg22892904	*CBX2, chromobox homolog 2*	11.48	0.068±0.006	0.607±0.051
cg24754277	*DAPK1, death-associated protein kinase 1*	28.34	0.115±0.005	0.708±0.049
cg21629895	*DNMT3A, DNA cytosine methyltransferase 3 alpha*	12.88	0.452±0.011	0.769±0.039
cg02932167	*ECEL1, endothelin converting enzyme-like 1*	17.57	0.115±0.007	0.672±0.059
cg25431974	*ECEL1, endothelin converting enzyme-like 1*	17.57	0.125±0.013	0.674±0.093
cg04515567	*FOXH1, forkhead box H1*	55.88	0.602±0.014	0.855±0.006
cg04464446	*GAL, galanin preproprotein*	194.63	0.241±0.022	0.735±0.056
cg00943909	*GNAS, guanine nucleotide binding protein*	47.33	0.076±0.016	0.528±0.081
cg27661264	*GNAS, guanine nucleotide binding protein*	47.33	0.037±0.005	0.355±0.054
cg18741908	*GPR160, G protein-coupled receptor 160*	60.48	0.068±0.006	0.466±0.038
cg20674521	*KCNJ4, potassium inwardly-rectifying channel J4*	6.11	0.306±0.024	0.772±0.043
cg21129531	*LRRC4, netrin-G1 ligand*	7.04	0.027±0.004	0.788±0.058
cg06144905	*PIPOX, L-pipecolic acid oxidase*	42.97	0.100±0.015	0.558±0.080
cg13083810	*POU5F1, POU domain; class 5;*	559.14	0.563±0.025	0.919±0.009
cg27377213	*PPP1R16B, protein phosphatase 1 regulatory inhibitor subunit 16B*	65.86	0.097±0.009	0.796±0.102
cg19580810	*RAB25, member RAS oncogene family*	6.16	0.062±0.010	0.703±0.030
cg09243900	*RAB25, member RAS oncogene family*	6.16	0.105±0.013	0.595±0.031
cg06303238	*SALL4, sal-like 4*	227.35	0.013±0.005	0.736±0.075
cg06614002	*SOX10, SRY-box 10*	5.23	0.028±0.005	0.829±0.046
cg01029592	*SOX15, SRY-box 15*	10.19	0.174±0.011	0.692±0.032
cg10242476	*TDGF1, teratocarcinoma-derived growth factor 1*	2472.59	0.146±0.013	0.387±0.052
cg20277416	*TM7SF2, transmembrane 7 superfamily member 2*	5.23	0.380±0.017	0.833±0.027
cg05656364	*VAMP8, vesicle-associated membrane protein 8*	9.69	0.070±0.010	0.698±0.081

Fold change of expression: Fold change of expression of the listed gene in human iPS/ES cells against the expression level in differentiated cells.

doi:10.1371/journal.pone.0013017.t003

Table 3 have trimethylation solely on K4 (Fig. 3C). Six genes have no histone trimethylation on K4 and K27 and the rest have bivalent K4/K27 trimethylation (Fig. 3C).

Discussion

Our genome-wide DNA methylation analysis shows that iPS and ES cells have similar methylation status although DNA methylation status of AM-iPS cells was closer to that of MRC-iPS cells than to that of ES cells in a small fraction. Doi et al. reported 71 differential methylated regions covering 64 genes between human iPS cells and ES cells [23]. Comparison of 535 aberrant DMSs (overlapping, 155; MRC-iPS specific, 125; AM-iPS specific, 255) with Doi's data, six genes that are *HOXA9*, *A2BP1*, *FZD10*, *SOX2*, *PTPRT* and *HYPK* overlapped. The inconsistency of most DMSs may be due to the stochastic nature of aberrant methylation through the genome. Human iPS and ES cells have general hyper-methylated status compared with differentiated cells. Our present genome-wide study indicates that pluripotent stem cells are generally hyper-methylated at promoter regions in comparison with differentiated cells. In the SS-DMRs, the number of CpG sites on non-CpG islands is grater than those on CpG islands, suggesting that promoter regions on non-CpG islands were more affected during reprogramming towards pluripotent stem cells. This result is consistent with the suggestion by Fouse et al. (2008) [24] that DNA methylation in mouse ES cells primarily occurred on non-CpG island regions of promoters.

Gene ontology analysis shows that signal transduction and transmembrane are major keywords for SS-hyper-DMRs. Most genes with SS-hyper-DMRs relate to differentiation. Recent studies demonstrate that blocking the p53 and TGFß pathways improves efficiency of generation of iPS cells [25,26,27,28,29,30]. Some genes related to these pathways are included in SS-hyper-DMR. Approximately 70% of SS-hyper-DMR have no modification of H3K4 and H3K27, suggesting that most genes with SS-hyper-DMRs are rigorously turned off by DNA methylation. By combining these findings with the result of *DNMT3A*, *DNMT3B* and *DNMT3L* induction in iPS/ES cells, we suggest that SS-hyper-DMRs apparently include genes that play a role in differentiated cells. Moreover, they must be silenced by DNMTs to establish pluripotency. We then identified 43 genes with SS-hyper-DMRs from "genes significantly suppressed in iPS/ES cells" (Table S3B and S4). In particular, *GBP3* and *SP100* could be used as epigenetic markers for pluripotency.

In addition, we successfully determined 23 genes with SS-hypo-DMRs from "genes significantly expressed in iPS/ES cells" (Table 3 and Table S3A). Those genes may start to be induced by demethylation and a significant subset of genes that act for de-

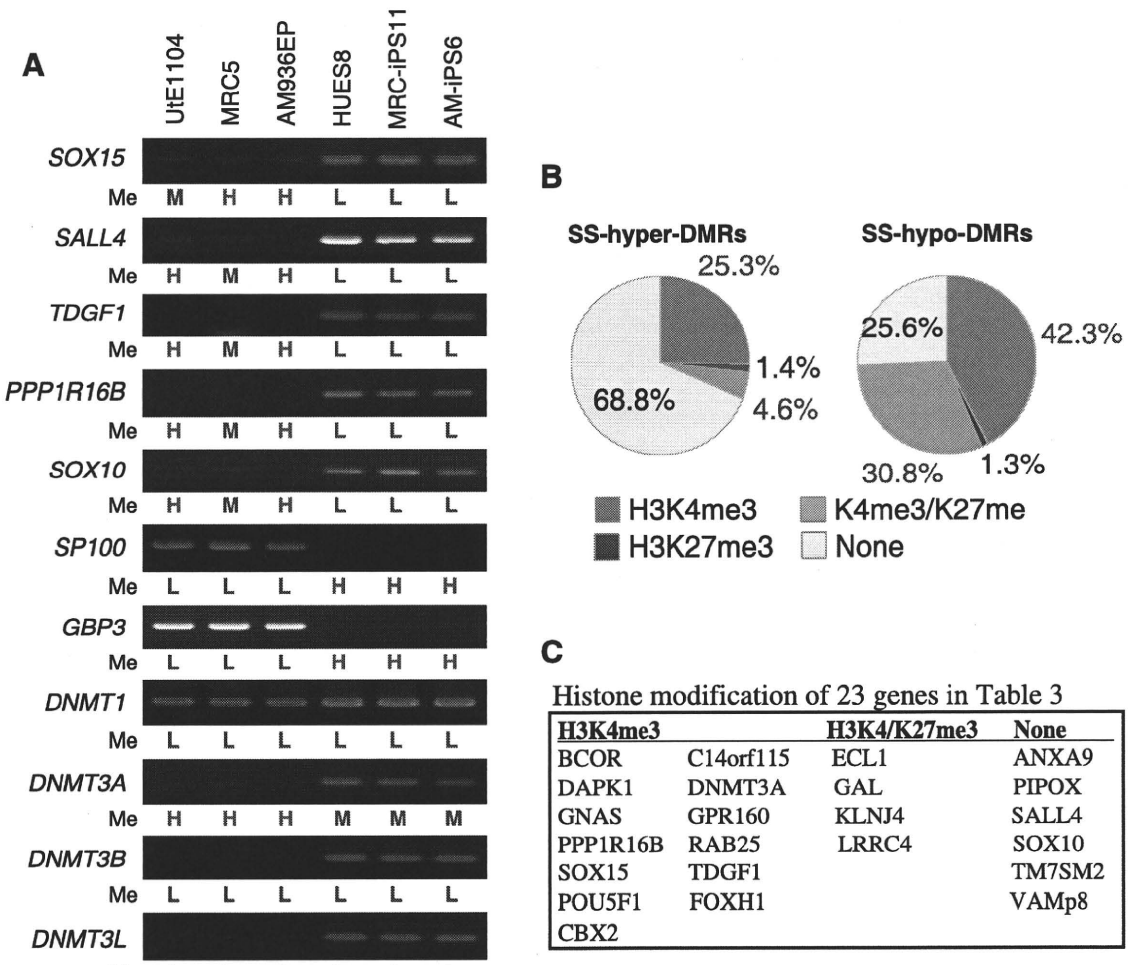

H3K4me3		H3K4/K27me3	None
BCOR	C14orf115	ECL1	ANXA9
DAPK1	DNMT3A	GAL	PIPOX
GNAS	GPR160	KLNJ4	SALL4
PPP1R16B	RAB25	LRRC4	SOX10
SOX15	TDGF1		TM7SM2
POU5F1	FOXH1		VAMp8
CBX2			

Figure 3. Expression and histone modification of the SS-DMRs related genes. (**A**) Expression patterns of representative genes. RT-PCR analysis of 7 representative genes and methyltransferase genes. Methylation levels (Me) of each promoter are shown under each panel. H = High methylation (0.7<score); M = Middle methylation (0.3<score≤0.7); L = Low methylation (score≤0.3). (**B**) Comparable distribution of the SS-DMR and histone trimethylation (me3) of H3K4 and H3K27. Percentage of H3K4me3, H3K27me3, bivalent H3K4me3/K27me3 or non-modification on genes in SS-hyper-DMRs and in SS-hypo-DMRs. (**C**) Histone modification of 23 genes in Table 3.
doi:10.1371/journal.pone.0013017.g003

differentiation escape methylation in pluripotent stem cells during global reprogramming. Promoters of most marker genes expressed in human iPS/ES cells were low methylated in all cells examined (Table S5C). Analysis of histone modification of H3K4me3 and K27me3 from the database suggested that expression of *DNMT3B* might be regulated by methylation of H3K4 but expression of *DNMT3L* might not be under control of histone modification of H3K4me3 and K27me3. Most genes with SS-hypo-DMRs without expression in human iPS/ES cells have modification of H3K4me, bivalent H3K4me/K27me, or none, but do not have H3K27me3 modification. These genes may therefore be ready to be activated upon differentiation.

These findings are in generally consistent with the previous reports that have compared methylation profiles in somatic cells, iPS cells, and ES cells [23,31,32]. However, their analyses were limited only to human fibroblasts as a source for generation of iPS cells. In this study, we analyzed human extra-embryonic amnion cells and iPS cells. The DNA methylation profile at promoter sites clearly distinguished human pluripotent stem cells from differentiated cells. The SS-DMRs defined in this experiment can be used as a signature for "stemness". In addition, knowledge of the DNA methylation profile in human ES and iPS cells derived from different cell types is absolutely imperative and may allow us to screen for optimum iPS/ES cells and to validate and monitor iPS/ES cell derivatives for human therapeutic applications.

Materials and Methods

Human Cells

Human endometrium, bone marrow stroma, auricular cartilage, extra finger bone marrow, amnion, placental artery endothelium and menstrual blood cells were collected by scraping tissues from surgical specimens as a therapy, under signed informed consent, with ethical approval of the Institutional Review Board of the National Institute for Child Health and Development, Japan. Signed informed consent was obtained from

donors, and the surgical specimens were irreversibly de-identified. All experiments handling human cells and tissues were performed in line with Tenets of the Declaration of Helsinki. Endometrium (UtE1104), bone marrow stroma (H4-1) [33], auricular cartilage (Mim1508E), extra finger bone marrow (Yub636BM), amnion (AM936EP), placental artery endothelium (PAE551) and menstrual blood cell (Edom22) [34] cell lines were independently established in our laboratory. H4-1, Mim1508E, Yub636BM, AM936EP, Edom22, and MRC-5 [35] cells were maintained in the POWEREDBY10 medium (MED SHIROTORI CO., Ltd, Tokyo, Japan). PAE551 were cultured in EGM-2MV BulletKit (Lonza, Walkersville, MD, USA) containing 5% FBS. Human induced pluripotent stem (iPS) cells were generated, via procedures described by Yamanaka and colleagues [2] with slight modification. Human iPS cell lines derived from MRC-5 were designated as MRC-iPS cells [13], also iPS cell lines from AM936EP were named as AM-iPS cells [12]. Human iPS cells were maintained in iPSellon medium (Cardio Incorporated, Osaka, Japan) supplemented with 10 ng/ml recombinant human basic fibroblast growth factor (bFGF, Wako Pure Chemical Industries, Ltd., Osaka, Japan). Frozen pellets of human ES cell (HUESCs) were kindly gifted from Drs. C. Cowan and T. Tenzan (Harvard Stem Cell Institute, Harvard University, Cambridge, MA).

Illumina Infinium HumanMethylation27 BeadChip assay

Genomic DNA was extracted from cells using the QIAamp DNA Mini Kit (Qiagen). One microgram of genomic DNA from each sample was bisulfite-converted using EZ DNA Methylation-Gold kit (Zymo Research), according to the manufacturer's recommendations. Bisulfite-converted DNA was hybridized to the HumanMethylation27 BeadChip (Illumina inc.). Methylation levels of each CpG site were determined with fluorescent signals for methylated and unmethylated alleles. Methylated and unmethylated signals were used to compute a Beta value, which was a quantitative score of DNA methylation levels ranging from "0", for completely unmethylated, to "1", for completely methylated. On the HumanMethylation27 BeadChip, oligonucleotides for 27,578 CpG sites covering more than 14,000 genes are mounted, mostly selected from promoter regions. 26,956 (97.7%) out of the 27,578 CpG sites are set at promoters and 20,006 (72.5%) sites are set on CpG islands. CpG sites with $\geq$0.05 "Detection p value" (computed from the background based on negative controls) were eliminated from the data for further analysis, leaving 24,949 valid for use with the 16 samples tested.

Analysis of DNA methylation data

To analyze DNA methylation data, we used the following web tools: TIGR MeV [36] (http://www.tm4.org/mev.html) for hierarchical clustering heat map, NIA Array [37] (http://lgsun.grc.nia.nih.gov/ANOVA/) for hierarchical clustering that classify DNA methylation data by similarity and for principal component analysis (PCA) that finds major component in data variability, DAVID Bioinformatics Resources [38] (http://david.abcc.ncifcrf.gov/home.jsp), PANTHER Classification System [39] (http://www.pantherdb.org/), WebGestalt [40] (WEB-based GEne SeT AnaLysis Toolkit) (http://bioinfo.vanderbilt.edu/webgestalt/) based on based on KEGG (Kyoto Encyclopedia of Genes and Genomes) database [41] (http://www.genome.jp/kegg/) for gene ontology analysis, the GEO database (http://www.ncbi.nlm.nih.gov/geo/) for surveying gene expression in human iPS/ES cells (accession no. GSE9832 [16] and GSE12583 [17]), and the UCSC Genome Browser website [42] (http://genome.ucsc.edu/).

RT-PCR

RNA was extracted from cells using the RNeasy Plus Mini kit (Qiagen). An aliquot of total RNA was reverse transcribed using random hexamer primers. The cDNA template was amplified using specific primers for *SOX10*, *SOX15*, *PPP1R16B*, *SALL4*, *TDGF1*, *Sp100* and *GBP3*. Expression of glyceraldehyde-3-phosphate dehydrogenase (GAPDH) was used as a positive control. Primers used in this study are summarized in Table S6A.

Quantitative combined bisulfite restriction analysis (COBRA) and bisulfite sequencing

To confirm DNA methylation state, bisulfite PCR-mediated restriction mapping (known as the COBRA method) was performed. Sodium bisulfite treatment of genomic DNA was carried out as described above. PCR amplification was performed using IMMOLASE^{TM} DNA polymerase (Bioline Ltd; London, UK) and specific primers (Table S6B). After digestion with restriction enzymes, HpyCH4IV or Taq I, quantitative-COBRA coupled with the Shimadzu MCE®-202 MultiNA platform (Shimadzu, Japan) known as the Bio-COBRA method was carried out for quantitative DNA methylation level. Information of primers and restriction enzyme is summarized in Table S6B. To determine the methylation status of individual CpG in *SOX15*, *SALL4*, *Sp100* and *GBP3*, the PCR product was gel extracted and subcloned into pGEM T Easy vector (Promega, Madison, WI), and then sequenced. Methylation sites were visualized and quality control was carried out by the web-based tool, "QUMA" (http://quma.cdb.riken.jp/) [43].

Supporting Information

Table S1 Frequency of methylation states in each cell line.
Found at: doi:10.1371/journal.pone.0013017.s001 (0.04 MB PDF)

Table S2 A list of genes with SS-hyper-DMRs and SS-hypo-DMRs on KEGG Pathway.
Found at: doi:10.1371/journal.pone.0013017.s002 (0.05 MB PDF)

Table S3 (A) DNA methylation states of 23 genes (26 CpG sites) in Table 3, (B) DNA methylation states of 43 genes (50 CpG sites) in Table S4.
Found at: doi:10.1371/journal.pone.0013017.s003 (1.61 MB PDF)

Table S4 A list of 43 genes with SS-hyper-DMRs exhibiting 'low' expression in human iPS/ES cells.
Found at: doi:10.1371/journal.pone.0013017.s004 (0.07 MB PDF)

Table S5 (A) DNA methylation states of DNA methyltransferases, (B) Histone methylation states of DNA methyltransferases, (C) DNA methylation states of marker genes in human iPS/ES cells.
Found at: doi:10.1371/journal.pone.0013017.s005 (0.57 MB PDF)

Table S6 (A) primers used for RT-PCR, and (B) primers used for COBRA.
Found at: doi:10.1371/journal.pone.0013017.s006 (0.52 MB PDF)

Data set S1 A list of overlapped aberrant DMSs.
Found at: doi:10.1371/journal.pone.0013017.s007 (0.16 MB XLS)

Data set S2 A list of MRC-iPS specific aberrant DMSs.

Found at: doi:10.1371/journal.pone.0013017.s008 (0.13 MB XLS)

Data set S3 A list of AM-iPS specific aberrant DMSs.
Found at: doi:10.1371/journal.pone.0013017.s009 (0.25 MB XLS)

Data set S4 A list of SS-hyper-DMRs.
Found at: doi:10.1371/journal.pone.0013017.s010 (0.61 MB XLS)

Data set S5 A list of SS-hypo-DMRs.
Found at: doi:10.1371/journal.pone.0013017.s011 (0.10 MB XLS)

References

1. Thomson JA, Itskovitz-Eldor J, Shapiro SS, Waknitz MA, Swiergiel JJ, et al. (1998) Embryonic stem cell lines derived from human blastocysts. Science 282: 1145–1147.
2. Takahashi K, Tanabe K, Ohnuki M, Narita M, Ichisaka T, et al. (2007) Induction of pluripotent stem cells from adult human fibroblasts by defined factors. Cell 131: 861–872.
3. Huangfu D, Osafune K, Maehr R, Guo W, Eijkelenboom A, et al. (2008) Induction of pluripotent stem cells from primary human fibroblasts with only Oct4 and Sox2. Nat Biotechnol 26: 1269–1275.
4. Dimos JT, Rodolfa KT, Niakan KK, Weisenthal LM, Mitsumoto H, et al. (2008) Induced pluripotent stem cells generated from patients with ALS can be differentiated into motor neurons. Science 321: 1218–1221.
5. Woltjen K, Michael IP, Mohseni P, Desai R, Mileikovsky M, et al. (2009) piggyBac transposition reprograms fibroblasts to induced pluripotent stem cells. Nature 458: 766–770.
6. Li E (2002) Chromatin modification and epigenetic reprogramming in mammalian development. Nat Rev Genet 3: 662–673.
7. Reik W (2007) Stability and flexibility of epigenetic gene regulation in mammalian development. Nature 447: 425–432.
8. Hattori N, Nishino K, Ko YG, Ohgane J, Tanaka S, et al. (2004) Epigenetic control of mouse Oct-4 gene expression in embryonic stem cells and trophoblast stem cells. J Biol Chem 279: 17063–17069.
9. Nishino K, Hattori N, Tanaka S, Shiota K (2004) DNA methylation-mediated control of Sry gene expression in mouse gonadal development. J Biol Chem 279: 22306–22313.
10. Zingg JM, Pedraza-Alva G, Jost JP (1994) MyoD1 promoter autoregulation is mediated by two proximal E-boxes. Nucleic Acids Res 22: 2234–2241.
11. Tada M, Takahama Y, Abe K, Nakatsuji N, Tada T (2001) Nuclear reprogramming of somatic cells by in vitro hybridization with ES cells. Curr Biol 11: 1553–1558.
12. Nagata S, Toyoda M, Yamaguchi S, Hirano K, Makino H, et al. (2009) Efficient reprogramming of human and mouse primary extra-embryonic cells to pluripotent stem cells. Genes Cells 14: 1395–1404.
13. Makino H, Toyoda M, Matsumoto K, Saito H, Nishino K, et al. (2009) Mesenchymal to embryonic incomplete transition of human cells by chimeric OCT4/3 (POU5F1) with physiological co-activator EWS. Exp Cell Res 315: 2727–2740.
14. Cowan CA, Klimanskaya I, McMahon J, Atienza J, Witmyer J, et al. (2004) Derivation of embryonic stem-cell lines from human blastocysts. N Engl J Med 350: 1353–1356.
15. Brena RM, Auer H, Kornacker K, Plass C (2006) Quantification of DNA methylation in electrofluidics chips (Bio-COBRA). Nat Protoc 1: 52–58.
16. Park IH, Zhao R, West JA, Yabuuchi A, Huo H, et al. (2008) Reprogramming of human somatic cells to pluripotency with defined factors. Nature 451: 141–146.
17. Aasen T, Raya A, Barrero MJ, Garreta E, Consiglio A, et al. (2008) Efficient and rapid generation of induced pluripotent stem cells from human keratinocytes. Nat Biotechnol 26: 1276–1284.
18. Sperger JM, Chen X, Draper JS, Antosiewicz JE, Chon CH, et al. (2003) Gene expression patterns in human embryonic stem cells and human pluripotent germ cell tumors. Proc Natl Acad Sci U S A 100: 13350–13355.
19. Barski A, Cuddapah S, Cui K, Roh TY, Schones DE, et al. (2007) High-resolution profiling of histone methylations in the human genome. Cell 129: 823–837.
20. Mikkelsen TS, Ku M, Jaffe DB, Issac B, Lieberman E, et al. (2007) Genome-wide maps of chromatin state in pluripotent and lineage-committed cells. Nature 448: 553–560.
21. Bibikova M, Laurent LC, Ren B, Loring JF, Fan JB (2008) Unraveling epigenetic regulation in embryonic stem cells. Cell Stem Cell 2: 123–134.
22. Zhao XD, Han X, Chew JL, Liu J, Chiu KP, et al. (2007) Whole-genome mapping of histone H3 Lys4 and 27 trimethylations reveals distinct genomic compartments in human embryonic stem cells. Cell Stem Cell 1: 286–298.
23. Doi A, Park IH, Wen B, Murakami P, Aryee MJ, et al. (2009) Differential methylation of tissue- and cancer-specific CpG island shores distinguishes human induced pluripotent stem cells, embryonic stem cells and fibroblasts. Nat Genet 41: 1350–1353.
24. Fouse SD, Shen Y, Pellegrini M, Cole S, Meissner A, et al. (2008) Promoter CpG methylation contributes to ES cell gene regulation in parallel with Oct4/Nanog, PcG complex, and histone H3 K4/K27 trimethylation. Cell Stem Cell 2: 160–169.
25. Hong H, Takahashi K, Ichisaka T, Aoi T, Kanagawa O, et al. (2009) Suppression of induced pluripotent stem cell generation by the p53-p21 pathway. Nature 460: 1132–1135.
26. Kawamura T, Suzuki J, Wang YV, Menendez S, Morera LB, et al. (2009) Linking the p53 tumour suppressor pathway to somatic cell reprogramming. Nature 460: 1140–1144.
27. Utikal J, Polo JM, Stadtfeld M, Maherali N, Kulalert W, et al. (2009) Immortalization eliminates a roadblock during cellular reprogramming into iPS cells. Nature 460: 1145–1148.
28. Marion RM, Strati K, Li H, Murga M, Blanco R, et al. (2009) A p53-mediated DNA damage response limits reprogramming to ensure iPS cell genomic integrity. Nature 460: 1149–1153.
29. Li H, Collado M, Villasante A, Strati K, Ortega S, et al. (2009) The Ink4/Arf locus is a barrier for iPS cell reprogramming. Nature 460: 1136–1139.
30. Maherali N, Hochedlinger K (2009) Tgfbeta Signal Inhibition Cooperates in the Induction of iPSCs and Replaces Sox2 and cMyc. Curr Biol 18: 1718–1723.
31. Bibikova M, Chudin E, Wu B, Zhou L, Garcia EW, et al. (2006) Human embryonic stem cells have a unique epigenetic signature. Genome Res 16: 1075–1083.
32. Deng J, Shoemaker R, Xie B, Gore A, LeProust EM, et al. (2009) Targeted bisulfite sequencing reveals changes in DNA methylation associated with nuclear reprogramming. Nat Biotechnol 27: 353–360.
33. Mori T, Kiyono T, Imabayashi H, Takeda Y, Tsuchiya K, et al. (2005) Combination of hTERT and bmi-1, E6, or E7 induces prolongation of the life span of bone marrow stromal cells from an elderly donor without affecting their neurogenic potential. Mol Cell Biol 25: 5183–5195.
34. Cui CH, Uyama T, Miyado K, Terai M, Kyo S, et al. (2007) Menstrual blood-derived cells confer human dystrophin expression in the murine model of Duchenne muscular dystrophy via cell fusion and myogenic transdifferentiation. Mol Biol Cell 18: 1586–1594.
35. Jacobs JP, Jones CM, Baille JP (1970) Characteristics of a human diploid cell designated MRC-5. Nature 227: 168–170.
36. Saeed AI, Sharov V, White J, Li J, Liang W, et al. (2003) TM4: a free, open-source system for microarray data management and analysis. Biotechniques 34: 374–378.
37. Sharov AA, Dudekula DB, Ko MS (2005) A web-based tool for principal component and significance analysis of microarray data. Bioinformatics 21: 2548–2549.
38. Huang da W, Sherman BT, Lempicki RA (2009) Systematic and integrative analysis of large gene lists using DAVID bioinformatics resources. Nat Protoc 4: 44–57.
39. Mi H, Lazareva-Ulitsky B, Loo R, Kejariwal A, Vandergriff J, et al. (2005) The PANTHER database of protein families, subfamilies, functions and pathways. Nucleic Acids Res 33: D284–288.
40. Zhang B, Kirov S, Snoddy J (2005) WebGestalt: an integrated system for exploring gene sets in various biological contexts. Nucleic Acids Res 33: W741–748.
41. Kanehisa M, Araki M, Goto S, Hattori M, Hirakawa M, et al. (2008) KEGG for linking genomes to life and the environment. Nucleic Acids Res 36: D480–484.
42. Kent WJ, Sugnet CW, Furey TS, Roskin KM, Pringle TH, et al. (2002) The human genome browser at UCSC. Genome Res 12: 996–1006.
43. Kumaki Y, Oda M, Okano M (2008) QUMA: quantification tool for methylation analysis. Nucleic Acids Res 36: W170–175.

Acknowledgments

We would like to express our sincere thanks to Drs. M. Yamada and K Miyado for discussion and critical reading of the manuscript, to Drs. C. Cowan and T. Tenzan for HUES cell lines, to Dr. D. Kami for establishing the PAE551 cell line, to K. Miyamoto for bisulfite sequencing, to Drs. K. Hata and K. Nakabayashi for COBRA.

Author Contributions

Conceived and designed the experiments: KN AU. Performed the experiments: KN MT MYI. Analyzed the data: KN YT. Contributed reagents/materials/analysis tools: KN MT MYI HM YF EC YM HO NK HA. Wrote the paper: KN AU.

Editorial Manager(tm) for In Vitro Cellular & Developmental Biology - Animal
Manuscript Draft

Manuscript Number:

Title: Induction of enamel matrix protein expression in an ameloblast cell line co-cultured with a mesenchymal cell line in vitro

Article Type: Articles (full research papers)

Keywords: ameloblastin; tooth differentiation; co-culture

Corresponding Author: Prof.Dr. Akiyoshi Taniguchi, Ph.D.

Corresponding Author's Institution: National Institute for Materials Science

First Author: Asako Matsumoto

Order of Authors: Asako Matsumoto; Hidemitsu Harada, Ph.D. DDS; Masahiro Saito, Ph.D. DDS; Akiyoshi Taniguchi, Ph.D.

Abstract: Interactions between epithelium and mesenchyme are important for organ and tissue development. In this study, in order to mimic interactions between epithelium and mesenchyme during native tooth development, we constructed three-dimensional culture systems in vitro using a collagen membrane. Two types of collagen membrane-based in vitro culture systems were constructed in which dental epithelial and dental follicle cell lines were cultured. One co-culture method involved inoculation of one cell line into one side of the collagen membrane, and the other cell line into the opposite side of the membrane (sandwich co-culture; SW). As a control, the second method involved culture of one of the cell lines on a culture dish and the second cell line on a collagen membrane, facing away from the first cell line (separate co-culture; SC). The HAT-7 cells were also grown as a monolayer culture on collagen. Ameloblast differentiation in these cultures was investigated by analysis of the mRNA and/or protein expression of ameloblastin and amelogenin. Our results suggest that interaction of epithelial and mesenchymal cells via the extracellular matrix is important for tooth differentiation in vitro. Our culture system should be a useful method for investigation of epithelial-mesenchymal interactions.

Induction of enamel matrix protein expression in an ameloblast cell line co-cultured with a mesenchymal cell line *in vitro*.

Asako Matsumoto[1,2,3], Hidemitsu Harada[4], Masahiro Saito[5] and Akiyoshi Taniguchi[1,2]

[1]Advanced Medical Materials Group, Biomaterials Center, National Institute for Materials Science, 1-1 Namiki, Tsukuba, Ibaraki 305-0044, Japan

[2]Biomaterials and Tissue Engineering, Graduate School of Comprehensive Human Science, University of Tsukuba, Tsukuba, Ibaraki 305-8572, Japan

[3]Kyokuto Pharmaceutical Industrial Co., Ltd. 3333-26 Aza-Asayama, Kamitezuna, Takahagi-shi, Ibaraki 318-0004, Japan

[4]Department of Oral Structure and Function Biology, Iwate Medical University, School of Dentistry, 1-3-27 Chuodori, Morioka, Iwate 020-8505, Japan

[5]Tissue Engineering Research Center, Tokyo University of Science, Noda, Chiba 278-8510, Japan

Keywords: ameloblastin, amelogenin, tooth differentiation, co-culture, ECM

Correspondence to: Akiyoshi Taniguchi

Biomaterials Center, National Institute for Materials Science, 1-1 Namiki, Tsukuba, Ibaraki 305-0044, Japan

Phone: +81-29-860-4505; Fax: +81-29-860-4714; E-mail: TANIGUCHI.Akiyoshi @nims.go.jp

Summary

Interactions between epithelium and mesenchyme are important for organ and tissue development. In this study, in order to mimic interactions between epithelium and mesenchyme during native tooth development, we constructed three-dimensional culture systems *in vitro* using a collagen membrane. Two types of collagen membrane-based *in vitro* culture systems were constructed in which dental epithelial and dental follicle cell lines were cultured. One co-culture method involved inoculation of one cell line into one side of the collagen membrane, and the other cell line into the opposite side of the membrane (sandwich co-culture; SW). As a control, the second method involved culture of one of the cell lines on a culture dish and the second cell line on a collagen membrane, facing away from the first cell line (separate co-culture; SC). The HAT-7 cells were also grown as a monolayer culture on collagen. Ameloblast differentiation in these cultures was investigated by analysis of the mRNA and/or protein expression of ameloblastin and amelogenin. Our results suggest that interaction of epithelial and mesenchymal cells via the extracellular matrix is important for tooth differentiation *in vitro*. Our culture system should be a useful method for investigation of epithelial-mesenchymal interactions.

Introduction

Epithelial cells communicate with epidermal cells through the extracellular matrix (ECM) to maintain and regulate highly differentiated functions. These interactions are thought to play an important role in the control of various characteristics of cells such as proliferation and differentiation. In order to mimic these interactions that occur in native tissue, three-dimensional culture systems have been created using various cell populations (Kurosawa et al. 2005; Ohno et al. 2008; Takayama et al. 2007) and reconstituted ECM (Takezawa et al. 2007). Co-culture models *in vitro* between two different cell types via reconstituted ECM have been developed for clarification of cell behavior associated with development, differentiation, regeneration, and pathogenesis *in vitro* (Gingras et al. 2003).

Tooth development is a classic instance of the process of epithelium-mesenchyme interactions and provides a useful experimental system for understanding the molecular mechanisms of organogenesis (Jernvall et al. 2000; Thesleff and Sharpe 1997). The early stage of tooth development is regulated by reciprocal interactions between epithelial and mesenchymal cells via cytokines such as transforming growth factor beta (TGFβ), fibroblast growth factor (FGF), and Leucine-Rich Amelogenin Protein (LRAP) [reviewed by (Thesleff and Mikkola 2002)], (Aberg et al. 1997; Thesleff and Mikkola 2002). Mesenchyme differentiates into odentoblasts which then form dentin. Epithelium differentiates into ameloblasts which secrete enamel matrix and form enamel. In the presecretory stage of tooth development, the dental epithelium and mesenchymal preodontoblasts are separated by the basement membrane matrix. [reviewed by (Thesleff and Hurmerinta 1981)].

Enamel matrix secreted by ameloblasts has been classified into two major

categories: amelogenin which makes up about 90% of the enamel extracellular matrix, and nonamelogenin including ameloblastin, enamelin, and tuftelin [reviewed by (Smith 1998)]. Ameloblastin, also known as amelin (Cerny et al. 1996) or sheathlin (Hu et al. 1997), and amelogenin are tooth-specific genes which play a critical role in proper tooth enamel formation (Fong et al. 1996; Fukumoto et al. 2004; Krebsbach et al. 1996; Xu et al. 2006a; Xu et al. 2006b). *In vitro* culture models that facilitate the study of epithelium-mesenchyme interactions are important for understanding tooth development at a molecular level. However, there is no useful model available that permits investigation of the molecular mechanism by which the ECM at sites of epithelial-mesenchymal interactions modulates tooth formation *in vitro*.

Collagen gels and matrigel often play important roles as scaffolds for reconstructing co-culture models. For example, endothelial cells form a network of branching tubular capillary-like structures into an overlaid collagen gel with embedded fibroblasts (Velazquez et al. 2002). The use of transparent collagen membranes has a number of advantages. It allows observation of the cells using a phase-contrast microscope, it can store cytokines and it is a simple culture method for three-dimensional culture systems (Orisaka et al. 2006).

In this study, we constructed three-dimensional culture systems *in vitro* using a collagen membrane for the co-culture of dental epithelial cells and dental follicle cells and gene and protein expression levels in these co-cultures were examined. Our results suggest that the interaction of epithelial and mesenchymal cells via the extracellular matrix is important for tooth differentiation *in vitro*.

Material and methods

Cells and Cell Cultures

The HAT-7 cells used in this study were derived from a dental epithelial cell line, which originated from the apical bud of a rat incisor (Kawano et al. 2002). The culture medium consisted of Dulbecco's modified Eagle's medium/F-12 (Invitrogen, Carlsbad, CA, USA) supplemented with 10% fetal bovine serum (FBS) and penicillin (100 units/ml)/streptomycin (100 μg/ml). The BCPb8 cells used were derived from a dental follicle cell line (a cementoblast progenitor), which originated from the follicle tissue of a bovine incisor (Saito et al. 2005). The culture medium consisted of α-minimum essential medium (α-MEM) supplemented with 10% FBS, penicillin (100 units/ml)/streptomycin (100 μg/ml), 50 mg/ml ascorbic acid and 2 mM L-glutamine (Invitrogen). All cultures were maintained in a humidified atmosphere of 5% CO_2 at 37 °C.

Co-culture using a transparent collagen membrane

Two different co-culture models were set up, both of which used the two dental cell lines and a transparent collagen membrane (Fig. 1). In the sandwich co-culture (SW) system one cell line was inoculated into one side of the collagen film in a culture dish and the second cell line was inoculated into the opposite side of the collagen film. (Orisaka et al. 2006). In the separate co-culture (SC) system, the BCPb8 cells were first seeded onto a 60 mm dish. After confirming microscopically that the BCPb8 cells had adhered to the dish, the dish and the transparent collagen membranes were washed with PBS. The HAT-7 cells (1×10^6 cells) were then seeded onto the collagen film inserted into the dish, on the side of the film facing away from the BCPb8 cells. The cells were

cultured in DMEM/F12 using 6.5 ml of medium per dish. The media were replaced with fresh media every two days. As a further control, HAT-7 cells were also grown in monolayer culture on a collagen film.

RNA Extraction and Real Time PCR Analysis

The mRNA levels of differentiation-related marker genes were determined using quantitative real-time PCR and species-specific primers (Kurosawa et al. 2005). Briefly, total RNA was extracted at various time points using ISOGEN (Nippon Gene, Tokyo, Japan). Three micrograms of total RNA was reverse-transcribed into cDNA using the SuperScript first-strand synthesis system (Invitrogen) according to the manufacturer's protocol.

Real-time PCR was performed using an ABI PRISM 7000 Sequence Detection System (Applied Biosystems, Foster City, CA, USA). A standard reaction was performed in a 96-well plate. This reaction was composed of 10 μl of SYBR Premix Ex TaqTM II (Takara, Siga, Japan), 10 pmol each of the forward and reverse primers, 1 μl of HAT-7 cDNA and distilled water to a final volume of 20 μl. The thermocycling conditions were 95 °C for 30 s, following by 40 cycles of 95 °C for 5 s and 60 °C for 34 s. Species-specific primers corresponding to a region of low-homology between rat and bovine cDNA were designed using Primer Express Software version 2.0 (Applied Biosystems) based on the sequence of the target gene. The data were normalized using expression of the housekeeping gene glyceraldehyde-3-phosphate dehydrogenase (GAPDH) as an endogenous control in the same reaction as the gene of interest. The primers used in this study were designated as follows: rat ameloblastin forward primer 5'-TTCACCCAAGGGAGGAGACTT-3, rat ameloblastin reverse primer

5'-CTCTCCTTTCTCAGGGCCTTTAGT-3', rat amelogenin forward primer 5'-TGGGAGCCCTGGTTATATCAA-3', rat amelogenin reverse primer 5'-GCTGCCTTATCATGCTCTGGT-A-3', rat GAPDH forward primer 5'-GCCCCCAACACTGAGCAT-3', rat GAPDH reverse primer, 5'-CCAGGCCCCTCCTGTTGT-3'.

Immunocytochemistry and immunohistochemistry

The surfaces of the cultured cells were washed three times with phosphate buffered saline (PBS) and the cells were fixed in 10% formalin for 10 min. After permeabilization with 0.5% Triton X-100 in PBS for 10 min, ameloblastin was stained using a polyclonal goat anti-ameloblastin antibody (1:50, Santa Cruz, Santa Cruz, CA, USA) for 1 h. After several washes with PBS containing 0.1% Tween 20 (Sigma, St. Louis, MO, USA), the cells were incubated with the secondary antibody, Alex-488-conjugated anti-goat IgG serum (1:200), for 1 h at room temperature. Nuclei were visualized by Hoechst 33258 (Wako, Osaka, Japan) staining. Confocal microscopy was performed using a Zeiss LSM 510 microscope (Carl Zeiss, Oberkochen, Germany).

Statistical Analysis

Result were presented as means ± standard deviation (n=3).SD. Date were statistically analyzed by Student t tests. $P < 0.05$ was regarded as significant.

Results

Interaction between epithelial and mesenchymal cells is important for tooth development. This interaction is mediated by the ECM, which acts as a cytokine store *in vivo*. It is therefore important to mimic ECM functions when constructing an *in vitro* co-culture system. We constructed two co-culture models to investigate the interaction between two different dental cell lines, a rat HAT-7 cell line that originated from dental epithelia, and bovine BCPb8 cells, derived from cementoblast progenitor cells (Fig. 1). One co-culture method, (sandwich co-culture; SW) cultured these cells by inoculation of the cell lines onto opposite sides of a collagen film suspended in a cell culture dish. The second, control method, termed "separate co-culture" (SC) cultured BCPb8 cells on the culture dish and the HAT-7 cells on a collagen film that faced away from the BCP8 cells on the dish.

To determine the gene expression levels of enamel matrix proteins quantitatively, we performed real-time PCR analysis using specific primers (Kurosawa et al. 2005). The specific rat primers used for this analysis were designed from regions of low-homology between rat and bovine cDNA to avoid cross-amplification. Glyceraldehyde-3-phosphate dehydrogenase mRNA expression in each cell line was used as an internal control. Ameloblastin mRNA expression in these culture systems is shown in Fig. 2. In the SW cells, the expression level of ameloblastin mRNA gradually increased after seeding of HAT-7 cells and continued to increase until at least day 14. The ameloblastin expression level was significantly increased on day 14 compared with the others condition such as SC culture, monolayer culture on a collagen membrane (ML). The degree of ameloblastin mRNA up-regulation in SC-cultured cells was less than that of SW-cultured cells on days 7 and 14. These results suggested that direct

interaction of HAT-7 and BCPb8 via the collagen membrane was important for tooth differentiation.

The expression of amelogenin mRNA in these culture systems is shown in Fig. 3. In the SW cells, the expression levels of amelogenin mRNA gradually increased after seeding of HAT-7 cells and continued to increase until at least day 14. On day 14, amelogenin expression was increased compared to HAT-7 cells grown in either monolayer culture or in SC method, although the difference compared to either control culture was not statistically significant. These results further suggest that direct interaction of HAT-7 and BCPb8 cells via a collagen membrane was important for tooth differentiation.

We next analyzed expression of the ameloblastin protein in the SW system by immunofluorescent staining using an anti-ameloblastin antibody, an Alexa 488-conjugated second antibody, and confocal laser scanning microscopy. The Alex488-Ameloblastin signal was detected in sandwich co-cultured HAT-7 cells from 3 days and had disappeared by day 14 (Fig. 4B, C and D). No ameloblastin signal was detected on day 1 of culture (Fig.4A). Ameloblastin protein expression was not detected in co-cultured BCPb8 cells on day 14 (Fig. 4E). These results indicate that HAT-7 cells can gradually differentiate into ameloblast-like cells in the SW system but not in the SC. These results suggest that interaction between HAT-7 and BCPb8 cells via a collagen membrane was important for tooth differentiation in protein expression level.

Discussion

We constructed and compared two *in vitro* culture systems both of which involved culture using a collagen membrane. Whereas, in both co-culture systems the two cell lines are exposed to soluble factors produced by both cell lines, only the SW co-culture system allows the two cell lines to physically contact each other through the collagen membrane. Our results showed that both the mRNA and protein expression of the ameloblastin were significantly increased in HAT-7 cells that were co-cultured with BCPb8 cells using the SW method. Soluble factors produced by the BCPb8 cells may also contribute to induction of ameloblastin expression. Furthermore, our data indicated that the collagen membrane might play a role, not only in the accumulation of, but also in the stabilization of, soluble factors from BCPb8 cells.

Although the soluble factors produced by BCPb8 cells that contribute to amelogenin expression have not been studied, they must be of relatively low molecular weight since only molecules with a molecular weight of less than 12.5 kDa can pass through the collagen membrane. Several soluble factors are known to be involved in the interaction between epithelial and mesenchymal tissue during tooth development including growth factors, cytokines and extracellular matrix molecules. Among these factors, the insulin-like growth factors (IGFs) have been proposed as autocrine/paracrine regulators of in vivo tooth development (Caton et al. 2005; Yamamoto et al. 2006) and the molecular weight of IGF is less than 12.5 kDa. Therefore, IGFs are promising candidate soluble factors for mediation of the stimulation of ameloblastin mRNA and protein expression in HAT-7 cells.

We reconstructed the interaction of dental epithelial and mesenchymal cells by co-culture of these cells using a collagen membrane *in vitro*. This method is easier to

perform than other methods of co-culture that use extracellular matrix components such as Matrigel. Using this method we were able to analyze cell signal transduction pathways that require dental epithelial and mesenchymal cell interactions. This study provides a useful tool for future analysis of epithelial-mesenchymal interactions.

Acknowledgments

This research was partially supported by the grant program "Collaborative Development of Innovative Seeds" from the Japan Science and Technology Agency (JST).

References

Aberg T, Wozney J, Thesleff I. 1997. Expression patterns of bone morphogenetic proteins (Bmps) in the developing mouse tooth suggest roles in morphogenesis and cell differentiation. Dev Dyn 210(4):383-96.

Caton J, Bringas P, Jr., Zeichner-David M. 2005. IGFs increase enamel formation by inducing expression of enamel mineralizing specific genes. Arch Oral Biol 50(2):123-9.

Cerny R, Slaby I, Hammarstrom L, Wurtz T. 1996. A novel gene expressed in rat ameloblasts codes for proteins with cell binding domains. J Bone Miner Res 11(7):883-91.

Fong CD, Slaby I, Hammarstrom L. 1996. Amelin: an enamel-related protein, transcribed in the cells of epithelial root sheath. J Bone Miner Res 11(7):892-8.

Fukumoto S, Kiba T, Hall B, Iehara N, Nakamura T, Longenecker G, Krebsbach PH, Nanci A, Kulkarni AB, Yamada Y. 2004. Ameloblastin is a cell adhesion molecule required for maintaining the differentiation state of ameloblasts. J Cell Biol 167(5):973-83.

Gingras M, Bergeron J, Dery J, Durham HD, Berthod F. 2003. In vitro development of a tissue-engineered model of peripheral nerve regeneration to study neurite growth. Faseb J 17(14):2124-6.

Hu CC, Fukae M, Uchida T, Qian Q, Zhang CH, Ryu OH, Tanabe T, Yamakoshi Y, Murakami C, Dohi N and others. 1997. Sheathlin: cloning, cDNA/polypeptide sequences, and immunolocalization of porcine enamel sheath proteins. J Dent Res 76(2):648-57.

Jernvall J, Keranen SV, Thesleff I. 2000. Evolutionary modification of development in mammalian teeth: quantifying gene expression patterns and topography. Proc Natl Acad Sci U S A 97(26):14444-8.

Kawano S, Morotomi T, Toyono T, Nakamura N, Uchida T, Ohishi M, Toyoshima K, Harada H. 2002. Establishment of dental epithelial cell line (HAT-7) and the cell differentiation dependent on Notch signaling pathway. Connect Tissue Res 43(2-3):409-12.

Krebsbach PH, Lee SK, Matsuki Y, Kozak CA, Yamada KM, Yamada Y. 1996. Full-length sequence, localization, and chromosomal mapping of ameloblastin. A novel tooth-specific gene. J Biol Chem 271(8):4431-5.

Kurosawa Y, Taniguchi A, Okano T. 2005. Novel method to examine hepatocyte-specific gene expression in a functional coculture system. Tissue Eng 11(11-12):1650-7.

Ohno M, Motojima K, Okano T, Taniguchi A. 2008. Up-regulation of drug-metabolizing enzyme genes in layered co-culture of a human liver cell line and endothelial cells. Tissue Eng Part A 14(11):1861-9.

Orisaka M, Mizutani T, Tajima K, Orisaka S, Shukunami K, Miyamoto K, Kotsuji F. 2006. Effects of ovarian theca cells on granulosa cell differentiation during gonadotropin-independent follicular growth in

cattle. Mol Reprod Dev 73(6):737-44.
Saito M, Handa K, Kiyono T, Hattori S, Yokoi T, Tsubakimoto T, Harada H, Noguchi T, Toyoda M, Sato S and others. 2005. Immortalization of cementoblast progenitor cells with Bmi-1 and TERT. J Bone Miner Res 20(1):50-7.
Smith CE. 1998. Cellular and chemical events during enamel maturation. Crit Rev Oral Biol Med 9(2):128-61.
Takayama G, Taniguchi A, Okano T. 2007. Identification of differentially expressed genes in hepatocyte/endothelial cell co-culture system. Tissue Eng 13(1):159-66.
Takezawa T, Nitani A, Shimo-Oka T, Takayama Y. 2007. A protein-permeable scaffold of a collagen vitrigel membrane useful for reconstructing crosstalk models between two different cell types. Cells Tissues Organs 185(1-3):237-41.
Thesleff I, Hurmerinta K. 1981. Tissue interactions in tooth development. Differentiation 18(2):75-88.
Thesleff I, Mikkola M. 2002. The role of growth factors in tooth development. Int Rev Cytol 217:93-135.
Thesleff I, Sharpe P. 1997. Signalling networks regulating dental development. Mech Dev 67(2):111-23.
Velazquez OC, Snyder R, Liu ZJ, Fairman RM, Herlyn M. 2002. Fibroblast-dependent differentiation of human microvascular endothelial cells into capillary-like 3-dimensional networks. Faseb J 16(10):1316-8.
Xu L, Harada H, Taniguchi A. 2006a. The exon 6ABC region of amelogenin mRNA contribute to increased levels of amelogenin mRNA through amelogenin protein-enhanced mRNA stabilization. J Biol Chem 281(43):32439-44.
Xu L, Harada H, Yokohama-Tamaki T, Matsumoto S, Tanaka J, Taniguchi A. 2006b. Reuptake of extracellular amelogenin by dental epithelial cells results in increased levels of amelogenin mRNA through enhanced mRNA stabilization. J Biol Chem 281(4):2257-62.
Yamamoto T, Oida S, Inage T. 2006. Gene expression and localization of insulin-like growth factors and their receptors throughout amelogenesis in rat incisors. J Histochem Cytochem 54(2):243-52.